CHEMISTRY
A EUROPEAN JOURNAL

ChemPubSoc
Europe

DOI: 10.1002/chem.201202602

Exploring the Reactivity of Multicomponent Photocatalysts: Insight into the Complex Valence Band of BiOBr

Yan-Fen Fang,[a] Wan-Hong Ma,[a] Ying-Ping Huang,*[a] and Gen-Wei Cheng[b]

Abstract: The band structure of multicomponent semiconductor photocatalysts, as well as their reactivity distinction under different wavelengths of light, is still unclear. BiOBr, which is a typical multicomponent semiconductor, may have two possible valence-band structures, that is, two discrete valence bands constructed respectively from O 2p and Br 4p orbitals, or one valence band derived from the hybridization of these orbitals. In this work, aqueous photocatalytic hydroxylation is applied as the probe reaction to investigate the nature and reactions of photogenerated holes in BiOBr. Three organic compounds (microcystin-LR, aniline, and benzoic acid) with different oxidation potentials were selected as substrates. Isotope labeling ($H_2{}^{18}O$ as the solvent) was used to determine the source of the O atom in the hydroxyl group of the products, which distinguishes the contribution of different hydroxylation pathways. Furthermore, a spin-trapping ESR method was used to quantify the reactive oxygen species (•OH and •OOH) formed in the reaction system. The different isotope abundances of the hydroxyl O atom of the products formed, as well as the reverse trend of the •OH/•OOH ratio with the oxidative resistance of the substrate under UV and visible irradiation, reveal that BiOBr has two separate valence bands, which have different oxidation ability and respond to UV and visible light, respectively. This study shows that the band structure of semiconductor photocatalysts can be reliably analyzed with an isotope labeling method.

Keywords: ESR spectroscopy · hydroxylation · isotopic labeling · photocatalysis · semiconductors

Introduction

Since Asahi and co-workers reported in 2001 that N-doped TiO_2 responds to visible light,[1] the difference in oxidative reactivity between visible- and UV-induced activation of multicomponent semiconductor photocatalysts has remained unclear.[2] Bismuth oxybromide (BiOBr), which has two kinds of anions (O^{2-} and Br^-) and responds to both UV and visible irradiation,[3] is an ideal system to investigate the band structure of multicomponent semiconductors and their reactivity under different wavelength regions of irradiation. BiOBr may have two plausible valence-band structures: 1) one valence band derived from the hybridization of O 2p and Br 4p orbitals, the activation of which by different wavelengths of light would lead to a hole ($h_{vb}{}^+$) with the same reactivity; and 2) two discrete valence bands constructed respectively by O 2p and Br 4p orbitals, which are excited by different wavelengths of light (O 2p to Bi 6p and Br 4p to Bi 6p) and have $h_{vb}{}^+$ with different oxidation potentials ($h_{O\,2p}{}^+$ and $h_{Bi\,6p}{}^+$).[4] Even though the catalyst has a band structure of the second kind, the interband relaxation of the $h_{vb}{}^+$ ($h_{O\,2p}{}^+$ to $h_{Br\,4p}{}^+$) would also lead to a single $h_{vb}{}^+$ type ($h_{Br\,4p}{}^+$) under both UV and visible irradiation (Figure 1), which makes the determination of the band structure very difficult.

In photocatalytic reactions, •OH is the most important radical intermediate. It is formed by the oxidation of H_2O

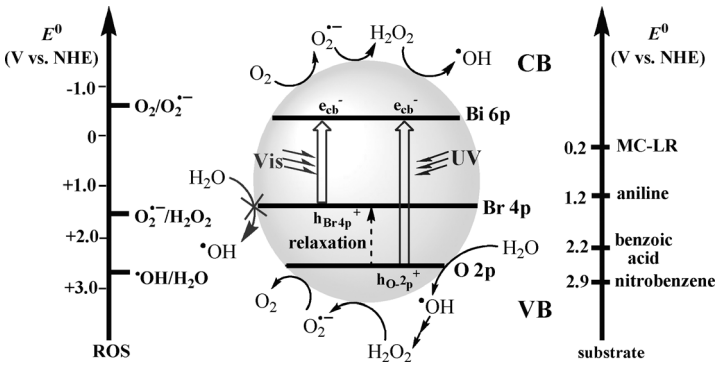

Figure 1. Potentials (versus normal hydrogen electrode, NHE) for the single-electron transfer of H_2O and O_2 and substrates used in this investigation, with corresponding reactions on the conduction band (CB) and valence band (VB) of activated BiOBr. No assumptions are made concerning the type of charge transfer involved. ROS = reactive oxygen species, MC-LR = microcystin-LR.

[a] Dr. Y.-F. Fang, Prof. W.-H. Ma, Prof. Y.-P. Huang
Engineering Research Centre of Eco-environment in Three Gorges Reservoir Region, Ministry of Education
China Three Gorges University, Hubei 443002 (P.R. China)
Fax: (+86) 717-639-7488
E-mail: huangyp@ctgu.edu.cn

[b] Prof. G.-W. Cheng
Institute of Mountain Hazards and Environment of Chinese Academy of Sciences
Chengdu 610041 (P.R. China)

Supporting information for this article is available on the WWW under http://dx.doi.org/10.1002/chem.201202602.

by h_{vb}^+ and the reduction of O_2 by the conduction-band electron (e_{cb}^-; see Figure 1). The ·OH formed via these two pathways attacks organic substrates identically.[5] The ·OH formed in reaction systems is typically quantified with the technique of spin-trapping electron spin resonance (ESR) spectroscopy. However, this method cannot distinguish the source of ·OH. Isotopic labeling provides a reliable method of analysis of the source and formation pathway of ·OH, that is, if the photocatalytic reaction is carried out in an oxygen isotope-labeled system ($H_2{}^{18}O/{}^{16}O_2$ or $H_2{}^{16}O/{}^{18}O_2$), the analysis of the isotope abundance in the hydroxylated product formed can determine the proportions of these two pathways of ·OH formation.

It has been proposed that, in aqueous photocatalytic systems, the hydroxylation of C–H moieties follows three possible pathways: 1) direct ·OH addition to form an OH-adduct radical, which is further oxidized to the product [Eq. (1)];[6a–c] 2) direct oxidation of substrate by h_{vb}^+ to form a cationic radical, which undergoes hydrolysis to yield the products [Eq. (2)];[6b,c] and 3) reaction of molecular O_2 with the cationic radical of the substrate to form an O_2 adduct, which further decomposes to the hydroxylated product [Eq. (3)].[6a,d]

$$RH + {}^{\bullet}OH \rightarrow {}^{\bullet}RHOH \rightarrow\rightarrow ROH \quad (1)$$

$$RH + h_{vb}^+ \rightarrow RH^{\bullet+} \xrightarrow{H_2O} \rightarrow ROH \quad (2)$$

$$RH^{\bullet+} \xrightarrow[-H^+]{O_2} ROO^{\bullet} \rightarrow\rightarrow ROH \quad (3)$$

Pathways (1) and (2) have been verified in various reaction systems; on the other hand, no experimental evidence corroborates that pathway (3) really works in photocatalysis. The products formed through pathway (2) have the hydroxyl O atom derived from H_2O. In contrast, the oxygen source of products formed through pathway (1) was uncertain, because ·OH can originate from either H_2O oxidation or O_2 (H_2O_2) reduction.

In this work, aqueous photocatalytic hydroxylation is applied as the probe reaction to investigate the nature and reactions of photogenerated h_{vb}^+ in BiOBr. Three organic compounds (microcystin-LR (MC-LR), aniline, and benzoic acid) with different redox potentials (Figure 1) were selected as substrates.[7] Isotopic labeling (with $H_2{}^{18}O$ as the solvent) was used to determine the source of the O atom in the hydroxyl group of the products. Reactive oxygen species (·OH and ·OOH) formed in the system were quantified by using an in situ spin-trapping ESR method. Our results reveal that BiOBr has two separate valence bands, the absorption edges of which are in the UV and visible region, respectively. The two valence-band holes generated have different oxidizing ability and induce different reactions.

Results and Discussion

In our previous study on the photocatalytic oxidation of MC-LR, epimeric products **a** and **b** (see Table 1), which are formed from the 1,2-dihydroxylation of the $C^6{=}C^7$ bond, were found to be the main intermediates.[8] Because two O atoms are added, three combinations of the origin of O atoms (both O atoms come from H_2O, both O atoms come from O_2, one O atom comes from H_2O and the other comes from O_2) are possible for each product. These combinations reflect the pathway of the reaction. We used the isotope labeling method to analyze the origin of added O atoms. The photocatalytic oxidation of MC-LR was carried out in $H_2{}^{18}O$ with $^{16}O_2$ in air as oxidant. The isotope abundance of the formed hydroxylated product was analyzed by HPLC–ESI-MS (Figure S1 in the Supporting Information). Because the possibility of isotopic exchange between the products and $H_2{}^{18}O$ was eliminated by control experiments, the oxygen isotope abundance of hydroxylated products clearly indicates the oxygen source. The measured isotope abundance was corrected with the natural isotope abundance to determine the origin of the hydroxyl O atoms (details are shown in the Supporting Information), and the results are displayed in Table 1. The reaction was also carried out in a TiO_2/UV system for comparison. When BiOBr is activated by UV light, about half of the hydroxyl O atoms come from O_2 (Table 1, entry 2, 49.9% for product **a** and 59.0% for product **b**). These data indicate that h_{vb}^+ and e_{cb}^- contribute equally to the reaction. The isotope abundance of the products formed in the TiO_2/UV system are nearly identical to those formed by BiOBr/UV (Table 1, entry 3, 54.1% for product **a** and 47.7% for product **b**). With TiO_2/UV photocatalysis, it is known that the ·OH initiating pathway (1) derives primarily from H_2O oxidation by h_{vb}^+ (in the valence band constructed with O 2p orbitals). However, this is not necessarily the case with BiOBr/UV because pathway (2), initiated by the direct oxidation of the substrate, can also generate products with hydroxyl O atoms derived from H_2O. In sharp contrast to UV irradiation, the activation of BiOBr by visible light yields products containing primarily O_2-derived O atoms (Table 1, entry 1, 81.4% for product **a** and 84.6% for product **b**). The difference between UV and visible-light irradiation indicates separate valence bands of BiOBr. Otherwise, the reactions induced by UV and visible light would be the same; that is, the h_{vb}^+ generated by irradiation with different wavelengths of light would all locate at the hybridized valence band and have the same reactivity. The different isotope abundance of the products formed in BiOBr/UV and BiOBr/Vis systems can be interpreted in two ways: 1) the production of ·OH from H_2O oxidation or 2) the direct oxidation of substrate is significantly inhibited when BiOBr is activated with visible instead of UV light.

The difference in oxygen source for MC-LR hydroxylation with UV versus visible excitation should be correlated with the oxidative reactivity of h_{vb}^+ in BiOBr. This assumption is confirmed by the hydroxylation of other substrates

Table 1. Isotopic abundances of the two oxygen atoms added to the $C^6{=}C^7$ bond in the hydroxylation of MC-LR in $H_2{}^{18}O$ and $^{16}O_2$ photocatalytic systems.[a]

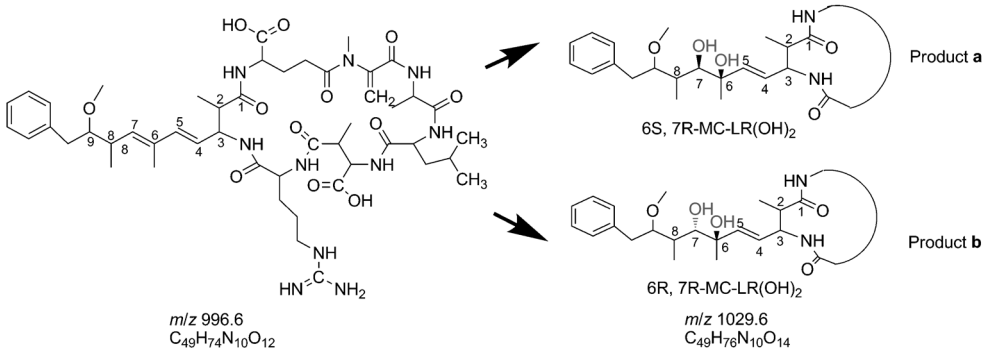

Entry	Conditions	Time [min]	Conv. [%]	Hydroxylation product **a** [%]				Hydroxylation product **b** [%]			
				$^{16}O^{16}O$	$^{16}O^{18}O$	$^{18}O^{18}O$	Total ^{16}O	$^{16}O^{16}O$	$^{16}O^{18}O$	$^{18}O^{18}O$	Total ^{16}O
1	BiOBr/Vis[b]	30	19.4	63.7	35.4	0.95	81.4	71.1	26.9	2.0	84.6
2	BiOBr/UV[b]	5	52.9	3.5	92.7	3.8	49.9	12.8	82.4	4.8	59.0
3	TiO_2/UV[c]	5	79.6	8.4	91.4	0.15	54.1	5.3	84.7	9.9	47.7

[a] $c_{MC\text{-}LR} = 5\ mg\,L^{-1}$, $H_2{}^{18}O$ (1 mL), under aerated ($^{16}O_2$) conditions. [b] BiOBr, $2\ g\,L^{-1}$. [c] P25 TiO_2, $2\ g\,L^{-1}$.

that are more resistant to oxidation than MC-LR (aniline and benzoic acid, see Table 2). According to Marcus's theory,[9] the rate of electron transfer is related to the standard free-energy change of the reaction, that is, the higher the oxidation potential of the substrate, the slower the oxidation. When aniline and benzoic acid were used as substrate, their direct oxidation was much slower than that of MC-LR. If the photogenerated $h_{vb}{}^+$ oxidizes primarily the substrate rather than H_2O (to $^{\bullet}OH$), its lifetime in the aniline and benzoic acid systems would be much longer than that in the MC-LR system. If BiOBr has separate valence bands, constructed with O 2p and Br 4p orbitals, respectively, the extending of the lifetime of $h_{vb}{}^+$ would make possible the interband relaxation of $h_{vb}{}^+$, that is, the $h_{vb}{}^+$ in the O 2p ($h_{O2p}{}^+$) band with strong oxidation ability converts to the Br 4p band and forms less oxidative $h_{Br4p}{}^+$. The interband relaxation of $h_{vb}{}^+$ would significantly reduce the difference between the UV and visible irradiation systems, since in both systems, $h_{Br4p}{}^+$, formed from direct excitation (visible system) or relaxation (UV system), initiates the oxidation of substrates. Experimental data confirmed this expectation; under both UV and visible-light irradiation, most of the hydroxyl O atoms (>90%) in the hydroxylated products of aniline and benzoic acid come from $^{16}O_2$ (Table 2, entries 1, 2, 4, and 5). In contrast, in the TiO_2/UV system, most of the hydroxyl O atoms in the hydroxylated products come from $H_2{}^{18}O$ (Table 2, entries 3 and 6). These results indicate that in BiOBr systems under both UV and visible-light irradiation, the $h_{vb}{}^+$-induced oxidation is of the same kind, and the oxidation ability is remarkably different from that of the $h_{vb}{}^+$ of TiO_2.

Table 2. Isotopic abundances of the hydroxyl O atoms in the monohydroxylated products formed in $H_2{}^{18}O$-labeled photocatalytic oxidation of aromatic compounds.[a]

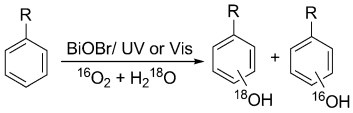

Entry	Substrate	Conditions	Time [h]	Conv. [%]	Abundance of ^{16}O [%]		
					para	*meta*	*ortho*
1		BiOBr/Vis	2.0	8.7	98.3	97.9	98.5
2	aniline[b]	BiOBr/UV	1.3	4.4	99.4	98.9	97.6
3		TiO_2/UV	3.0	61.0	48.0	48.0	70.1
4		BiOBr/Vis	3.0	4.4	98.0	98.9	90.7
5	benzoic acid[c]	BiOBr/UV	0.3	5.9	93.0	98.2	91.4
6		TiO_2/UV	2.0	17.0	21.0	10.3	20.1
7[e]		BiOBr/Vis	2.0	–	–	–	–
8[e]	nitrobenzene[d]	BiOBr/UV	1.5	–	–	–	–
9[f]		TiO_2/UV	2.0	–	53.4	50.3	62.0

[a] $H_2{}^{18}O$ suspension (1 mL) containing $2\ g\,L^{-1}$ photocatalyst (BiOBr or TiO_2), under aerated ($^{16}O_2$) conditions. [b] The initial concentration of aniline was 50 mM. [c] The initial concentration of BA was 20 mM. [d] The initial concentration of NB was 50 mM. [e] No substrate conversion or product formation was observed. [f] The conversion of substrate was too low to be quantified.

The ^{16}O abundances of the hydroxylated products of aniline and benzoic acid are considerably higher than that of MC-LR (Table 1). The close isotope abundances of the hydroxylated products for the BiOBr/UV and BiOBr/Vis systems when aniline or benzoic acid was used as substrate are also in contrast to the oxidation of MC-LR. These differences among MC-LR, aniline, and benzoic acid systems illustrate that the $h_{vb}{}^+$ initiate the hydroxylation of substrates primarily through the direct oxidation of the substrate [pathway (2)], rather than the oxidation of H_2O to $^{\bullet}OH$ [initiating pathway (1)], otherwise the oxidative susceptibility of substrates cannot affect the oxygen source for the hydroxylated product. If the oxidation potential of the substrate is much higher than that of the valence band of O 2p, the substrate cannot be oxidized by $h_{vb}{}^+$. The oxidation of H_2O is also limited by the rapid $h_{O2p}{}^+ \rightarrow h_{Br4p}{}^+$ relaxation. Therefore, the reaction of $h_{vb}{}^+$ is completely im-

peded, and the catalytic cycle, including the reduction of O_2 by e_{cb}^- to $^{\bullet}OH$, would shut down. Indeed, when nitrobenzene ($E^0 = 2.9$ V vs. NHE) was used as the substrate (Table 2, entries 7 and 8), neither visible nor UV irradiation induced the oxidation of the substrate. In contrast, even though direct oxidation of nitrobenzene by the h_{vb}^+ of TiO_2 is also not viable ($E_{vb} = 2.7$ V),[6b] nitrobenzene can be oxidized in the TiO_2/UV system, forming hydroxylated products with approximately 50% ^{18}O. This can be attributed to the oxidation of H_2O by h_{O2p}^+ (cannot relax as in the case of BiOBr) to produce $^{\bullet}OH$, which induces the hydroxylation of nitrobenzene (Table 2, entry 9).

To further explore the activation of H_2O and O_2 in the BiOBr system, spin-trapping ESR spectroscopy was used to detect the radicals (specifically $^{\bullet}OH$ and $^{\bullet}OOH$) formed during the hydroxylation of MC-LR, aniline, and benzoic acid (Figure 2). The typical signals of the trapped $^{\bullet}OH$ and $^{\bullet}OOH$ were measured in these systems, but their intensity altered with the light source, substrate, and irradiation time. Aniline and benzoic acid, which are more difficult to oxidize, gave weaker ESR intensities for both $^{\bullet}OH$ and $^{\bullet}OOH$ relative to those for MC-LR. The $^{\bullet}OH$ is produced from two sources, the reduction of O_2 (H_2O_2) and the oxidation of H_2O, whereas $^{\bullet}OOH$ is formed exclusively from molecular O_2.[5a] The ratio of $^{\bullet}OH$ to $^{\bullet}OOH$ indicates the relative amounts of H_2O and O_2 activated. Although the absolute quantification of $^{\bullet}OH$ and $^{\bullet}OOH$ by ESR spectroscopy is difficult, a comparison of the $^{\bullet}OH/^{\bullet}OOH$ ratio for each substrate reaction under both UV and visible-light irradiation is realistic and significant for understanding the initial activation step on BiOBr (Figure 3).

During MC-LR hydroxylation by BiOBr under visible light, the signal of trapped $^{\bullet}OOH$ was very weak and the $^{\bullet}OH$ signal relatively strong ($^{\bullet}OH/^{\bullet}OOH = 8$). However, a significant decrease of the $^{\bullet}OH/^{\bullet}OOH$ ratio (to 0.9 and 0.7, respectively) occurred for both aniline and benzoic acid under similar conditions, that is, the easier the oxidation of the substrate, the larger the $^{\bullet}OH/^{\bullet}OOH$ ratio. Considering that H_2O_2 is a key intermediate in O_2 reduction, and that $^{\bullet}OH$ derives primarily from the reduction of O_2 (via H_2O_2), we attribute this phenomenon to the reduction of H_2O_2 by e_{cb}^-. As noted above, a substrate more easily oxidized would increase the rate of h_{vb}^+ capture, inhibit the h_{vb}^+–e_{cb}^- recombination, and then facilitate the reduction of H_2O_2 to $^{\bullet}OH$ by e_{cb}^-. Therefore, the $^{\bullet}OH/^{\bullet}OOH$ ratio would increase with the oxidative susceptibility of the substrate.

Under UV irradiation, the distribution of radicals is converse to that of the BiOBr/Vis system, that is, the $^{\bullet}OH/^{\bullet}OOH$ ratio increases dramatically with the substrate resist-

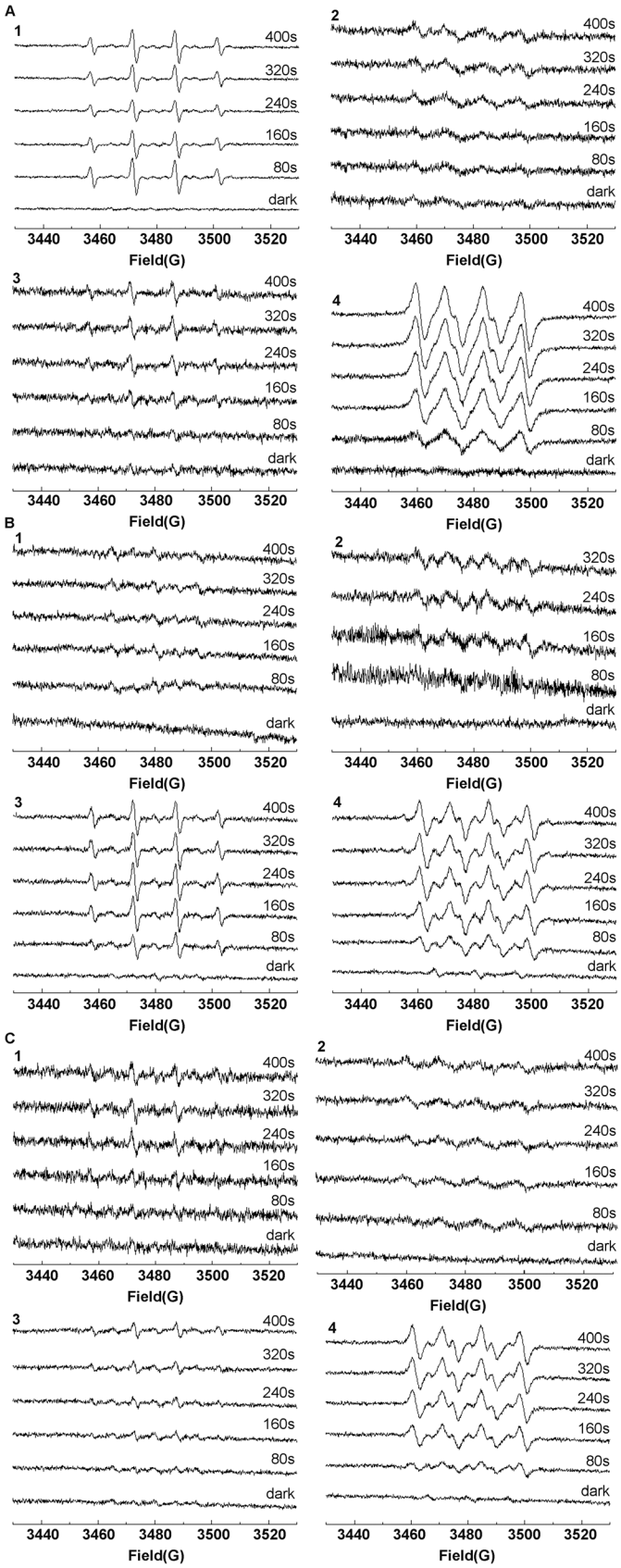

Figure 2. ESR signals of the dimethylpyrrolidine 1-oxide (DMPO)–$^{\bullet}OH$ and DMPO–$^{\bullet}OOH$ adducts in aqueous solution (panels 1 and 3) and method solution (panels 2 and 4). Panels 1 and 2 were under visible-light irradiation and panels 3 and 4 were under UV-light irradiation in the substrate/BiOBr system. A) MC-LR; B) aniline; C) benzoic acid. Reaction conditions: MC-LR, 3.0 mg mL^{-1}; BiOBr, 10 mg mL^{-1}; benzoic acid, 0.1 mM; aniline, 0.1 mM; DMPO, 0.4 mol L^{-1}.

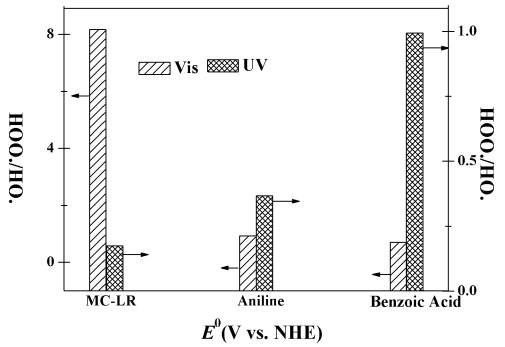

Figure 3. Intensity ratio of ·OH/·OOH versus redox potential of the substrate, obtained by using ESR spectroscopy with DMPO spin trapping. Reaction conditions are the same as in Figure 2.

ance to oxidation (·OH/·OOH is 0.18 for MC-LR, 0.37 for aniline, and 0.99 for benzoic acid, Figure 3). The very small ·OH/·OOH ratio for MC-LR, relative to that of the visible-light system, is explained by the production of high-energy h_{O2p}^+ in the BiOBr/UV system. As shown in Figure 1, h_{O2p}^+ can oxidize H_2O_2 (from O_2 reduction) to ·OOH. This process would facilitate the formation of ·OOH, and inhibit the formation of ·OH (mainly from the reduction of H_2O_2) through competitive consumption of H_2O_2. As the substrate becomes more difficult to oxidize, due to the relaxation of h_{O2p}^+ to h_{Br4p}^+, the effect of h_{O2p}^+ on ·OH and ·OOH would diminish. As a result, a higher ·OH/·OOH ratio was measured in the systems of aniline and benzoic acid.

Conclusion

Hydroxylation reactions, photocatalyzed by BiOBr under both UV and visible light, were investigated by using ^{18}O isotopic labeling. The correlation of ·OH/·OOH ratio with substrate redox potential in both systems was measured and analyzed. Our results show that BiOBr has two separate valence bands, which are constructed with O 2p and Br 4p orbitals, respectively, instead of a hybridized valence band. These two valence bands respond respectively to UV and visible irradiation and display complex reactivity. To the best of our knowledge, this is the first example of the existence of separate valence bands in a semiconductor that has been determined experimentally.

Experimental Section

Materials: BiOBr (surface area, ca. 13 $m^2 g^{-1}$, JCPDS card no. 78-0348) was prepared. Microcystin-LR (MC-LR) was purchased from Express Technology Company. $H_2{}^{18}O$, from Jiangsu Changshu Chemical Limited, had an initial isotopic enrichment of 85.6% as determined by mass spectrometry. Other chemicals were of reagent grade and used without further purification. Deionized and doubly distilled water was used throughout this study.

Photocatalysis: The light sources used were a 500 W halogen lamp and a 100 W mercury lamp (Institute of Electric Light Source, Beijing, China) positioned inside a cylindrical Pyrex reactor and surrounded by a circulating-water jacket for cooling. To ensure illumination by only visible light, a cutoff filter was placed outside the Pyrex jacket to completely eliminate any radiation at wavelengths below 420 nm. Similarly, a UV-365 filter was used to avoid direct photolysis from ultraviolet B and C radiation. Prior to the irradiation, the suspensions were stirred magnetically in the dark for approximately 2 h to ensure the establishment of an adsorption/desorption equilibrium. Microcystin-LR (3.0 mg L^{-1}, 10 mL; Express Technology Co., China) and catalyst powders (2 mg) were placed in a Pyrex vessel. At a given time, the solution (300 μL) was collected, centrifuged, and then filtered through a Millipore filter (pore size 0.22 μm) to remove the solid catalyst particles. The solution pH was 6.25.

Analysis: The oxygen isotope abundance of the hydroxylated product was analyzed by HPLC–ESI-MS (Agilent LC 1200/Ion Trap 6310) with a C-18 column (250 m × 2.1 mm). Each measurement was repeated at least three times to ensure accuracy. Figure S1 in the Supporting Information gives the typical ESI-MS spectra (acquired by UV and MS detectors) of the substrate. The measured isotope abundance of the product was corrected with the oxygen isotope abundance of solvent H_2O and the natural isotope abundance of the product by use of Equations (4) and (5), in which C_p, C_n, and C_w are the ^{18}O percentages of the measured isotope abundance of the product, natural isotope abundance of the product, and measured isotope abundance of solvent H_2O, respectively.

$$H_2O\% = \frac{C_p - C_n}{C_w - C_n} \times 100 \quad (4)$$

$$O_2\% = \frac{C_w - C_p}{C_w - C_n} \times 100 \quad (5)$$

EPR spin-trap analysis: A Brucker EPR spectrometer (model E500) equipped with a Quanta-Ray Nd:YAG laser (355 and 532 nm) was used for measuring the electron spin resonance (ESR) signals of ·OH and $O_2^{\cdot-}$ spin-trapped by dimethylpyrrolidine 1-oxide (DMPO). To minimize experimental errors, the same quartz capillary tube was used for all ESR measurements.

Acknowledgements

We thank Dr. David M. Johnson of Ferrum College (Ferrum, VA) and Dr. Li Yue of Nankai University (Tianjin, P.R. China) for their assistance in revising the manuscript. This work was funded by the National Natural Science Foundation of China (No. 21177072 and 21207079), the National Basic Research Program of China (No. 2008CB417206) and the Youth Scientific Research Funds (No. 65121003).

[1] R. Asahi, T. Morikawa, T. Waki, K. Aoki, Y. Taga, *Science* **2001**, *293*, 269–271.
[2] a) C. Gomes Silva, R. Juárez, T. Marino, R. Molinari, H. Garcia, *J. Am. Chem. Soc.* **2011**, *133*, 595–602; b) H. Park, W. Y. Choi, *J. Phys. Chem. B* **2005**, *109*, 11667–11674; c) X. H. Wang, J. G. Li, H. Kamiyama, Y. Moriyoshi, T. Ishigaki, *J. Phys. Chem. B* **2006**, *110*, 6804–6809; d) J. M. Herrmann, J. Disdier, P. Pichat, *Chem. Phys. Lett.* **1984**, *108*, 618–622.
[3] a) X. Chang, J. Huang, C. Cheng, Q. Sui, W. Sha, G. Ji, S. Deng, G. Yu, *Catal. Commun.* **2010**, *11*, 460–464; b) J. Henle, P. Simon, A. Frenzel, S. Scholz, S. Kaskel, *Chem. Mater.* **2007**, *19*, 366–373; c) J. Zhang, F. J. Shi, J. Lin, D. F. Chen, J. M. Gao, Z. X. Huang, X. X. Ding, C. Tang, *Chem. Mater.* **2008**, *20*, 2937–2941; d) Z. H. Ai, W. K. Ho, S. C. Lee, L. Z. Zhang, *Environ. Sci. Technol.* **2009**, *43*, 4143–4150; e) X. Zhang, Z. H. Zhi, F. Jia, L. Z. Zhang, *J. Phys. Chem. C* **2008**, *112*, 747–753.
[4] W. L. Huang, Q. Zhu, *J. Comput. Chem.* **2009**, *30*, 183–190.
[5] a) M. R. Hoffmann, S. T. Martin, W. Choi, D. W. Bahnemann, *Chem. Rev.* **1995**, *95*, 69–96; b) M. A. Fox, M. T. Dulay, *Chem. Rev.* **1993**,

93, 341–357; c) C. Chen, W. Ma, J. Zhao, *Chem. Soc. Rev.* **2010**, *39*, 4206–4219.
[6] a) T. D. Bui, A. Kimura, S. Ikeda, M. Matsumura, *J. Am. Chem. Soc.* **2010**, *132*, 8453–8458; b) Y. Li, B. Wen, C. Yu, C. Chen, H. Ji, W. Ma, J. Zhao, *Chem. Eur. J.* **2012**, *18*, 2030–2039; c) S. Goldstein, G. Czapski, J. Rabani, *J. Phys. Chem.* **1994**, *98*, 6586–6591; d) G. A. Russell, *J. Am. Chem. Soc.* **1957**, *79*, 3871–3877.
[7] a) T. Tachikawa, M. Fujitsuka, T. Majima, *J. Phys. Chem. C* **2007**, *111*, 5259–5275; b) A. V. Humble, G. M. Gadd, G. A. Codd, *Water Res.* **1997**, *31*, 1679–1686; c) M. Jonsson, J. Lind, T. Reitberger, T. E. Eriksen, G. Merenyi, *J. Phys. Chem.* **1993**, *97*, 11278–11282; d) C. Hansch, A. Leo, R. W. Taft, *Chem. Rev.* **1991**, *91*, 165–195.
[8] F. Yanfen, H. Yingping, Y. Jing, W. Pan, C. Genwei, *Environ. Sci. Technol.* **2011**, *45*, 1593–1600.
[9] a) R. A. Marcus, *J. Phys. Chem. C* **2009**, *113*, 14598–14608; b) P. Kebarle, S. Chowdhury, *Chem. Rev.* **1987**, *87*, 513–534.

Received: July 24, 2012
Revised: November 8, 2012
Published online: January 16, 2013

